Applications in Energy and Combustion Science 17 (2024) 100232

Contents lists available at ScienceDirect

Applications in Energy and Combustion Science

journal homepage: www.sciencedirect.com/journal/applications-in-energy-and-combustion-science

Development of manganese-iron mixed oxides reinforced with titanium and prepared from minerals for their use as oxygen carriers

Beatriz Zornoza [a,b], Teresa Mendiara [b,*], Alberto Abad [b]

[a] Chemical and Environmental Engineering Department, Instituto de Nanociencia y Materiales de Aragón (INMA), Universidad de Zaragoza-CSIC, Zaragoza 50018, Spain

[b] Instituto de Carboquímica (ICB-CSIC), Miguel Luesma Castán, 4, Zaragoza 50018, Spain

ARTICLE INFO

Keywords:
CO_2 capture
Chemical looping
Low-cost
Manganese-iron oxides
Magnetic support
titanium oxide

ABSTRACT

Chemical Looping Combustion (CLC) allows CO_2 capture at low cost. This technology is based on solid oxygen carriers which supply the oxygen required for combustion of the fuel while they experience successive reduction-oxidation cycles. Oxygen carriers based on minerals or industrial residues present the advantage of their low cost but complete combustion of the fuel is not always achieved. Manganese-iron mixed oxides doped with titanium can improve combustion efficiency due to its oxygen uncoupling capability. Moreover, they present the advantage of their magnetic properties. The objective of this work was to produce this type of oxygen carriers from minerals/residues instead of from synthetic materials. Four oxygen carriers with a fixed Mn-Fe molar ratio were produced with a 7 wt.% TiO_2 addition. Two manganese-based (MnSA and MnGBMPB) and one iron-based (Tierga) minerals were used as source of Mn and Fe, respectively. As source of Ti, the mineral ilmenite was used. After characterization of the materials, their reactivity was analysed in a TGA. The reactivity to the main combustion gasses was lower than that corresponding to similar oxygen carriers obtained from synthetic sources although they maintained their magnetic properties. Thus, its use as magnetic support of oxygen carriers was recommended. In this respect, first tests were conducted using CuO as active phase supported on one of the low-cost support materials produced in this work.

1. Introduction

The European Union (EU) has set the objective to be climate-neutral by 2050 which implies net-zero greenhouse gas emissions. This objective is the core of the European Green Deal [1] and it aligns with the global climate action under the Paris Agreement [2]. Becoming climate neutral means reducing greenhouse gas emissions as much as possible, but also compensating for any remaining emissions. Carbon capture and storage (CCS) is one of the technologies capable of achieving both objectives. CCS involves the capture of CO_2, from large point sources like power generation facilities that use either fossil fuels or biomass as fuel, delivering negative CO_2 emissions with bioenergy (BECCS) in the latter case. CCS can tackle emissions in hard-to-abate sectors, particularly heavy industries like cement, steel or chemicals. CCS also enables low-carbon hydrogen production, which can support the decarbonisation of other parts of the energy system, such as industry, trucks and ships [3].

Chemical Looping Combustion (CLC) is an advanced CCS technology which could play a significant role in addressing the cutting of CO_2 emissions since it significantly reduces the energy penalty associated to carbon capture [4]. CLC has experienced a significant development in the last decades, covering a wide range of fuels [5]. In the CLC concept, the oxygen required for the combustion of the fuel is supplied by a solid oxygen carrier [6] circulating between two interconnected reactors. Thus, the direct contact between fuel and air is avoided and the capture of the CO_2 generated during combustion is intrinsic to the process. Fig. 1 shows the scheme of the CLC process.

In the fuel reactor, the fuel is oxidized to CO_2 and H_2O while the oxygen carrier is reduced. Then, it is transferred to the air reactor where it is regenerated in air. Nevertheless, the energy released is the same as in conventional combustion of the fuel.

The cornerstone in the advance of CLC is the development of adequate oxygen carriers. Metal oxides based on nickel, copper, iron and manganese have been extensively tested as oxygen carriers for CLC, together with mixed oxides formed as combination of the previous and also perovskite-type materials [7]. CLC oxygen carriers should present a

* Corresponding author.
E-mail address: tmendiara@icb.csic.es (T. Mendiara).

https://doi.org/10.1016/j.jaecs.2023.100232
Received 13 September 2023; Received in revised form 6 December 2023; Accepted 8 December 2023
Available online 12 December 2023
2666-352X/© 2023 The Authors. Published by Elsevier Ltd. This is an open access article under the CC BY-NC-ND license (http://creativecommons.org/licenses/by-nc-nd/4.0/).

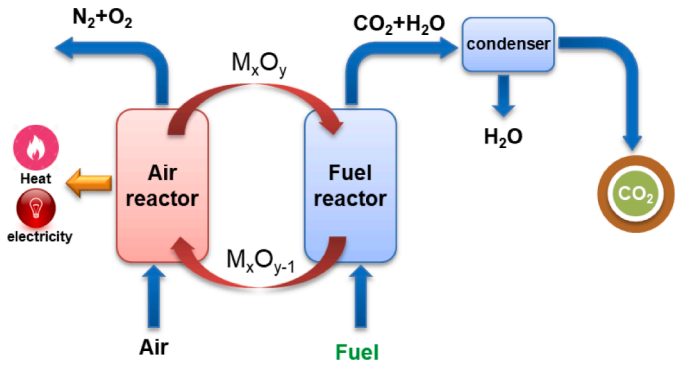

Fig. 1. Scheme of the CLC process.

compendium of properties to be considered suitable. Among the most important, sufficient reactivity/selectivity and a high lifetime, in addition to being environmentally sustainable.

Manganese-iron mixed oxides were identified as suitable oxygen carriers for the CLC process [8–10,]. Their cost is not comparable to that of nickel or copper or even more complex perovskites. Moreover, they present an interesting property which is the fact that they show magnetic properties in the spinel phase, which makes them especially applicable to the combustion of fossil fuels.

Manganese-iron mixed oxides allow the combustion of a fuel by two mechanisms in parallel. One of the mechanism implies reaction with gaseous oxygen released (oxygen uncoupling) when bixbyite phase, $(Mn_xFe_{1-x})_2O_3$, is reduced to spinel phase, $(Mn_xFe_{1-x})_3O_4$.

$$3\ (Mn_xFe_{1-x})_2O_3 \leftrightarrow 2\ (Mn_xFe_{1-x})_3O_4 + 0.5\ O_2 \quad (r1)$$

The other implies reaction with lattice oxygen when bixbyite phase (BIX) is reduced to spinel phase (SP), and then to manganowüstite phase (MW), $(Mn_xFe_{1-x})O$:

$$3\ (Mn_xFe_{1-x})_2O_3 + H_2 \rightarrow 2\ (Mn_xFe_{1-x})_3O_4 + H_2O \quad (r2)$$

$$3\ (Mn_xFe_{1-x})_2O_3 + CO \rightarrow 2\ (Mn_xFe_{1-x})_3O_4 + CO_2 \quad (r3)$$

$$12\ (Mn_xFe_{1-x})_2O_3 + CH_4 \rightarrow 8\ (Mn_xFe_{1-x})_3O_4 + CO_2 + 2\ H_2O \quad (r4)$$

$$(Mn_xFe_{1-x})_3O_4 + H_2 \rightarrow 3\ (Mn_xFe_{1-x})O + H_2O \quad (r5)$$

$$(Mn_xFe_{1-x})_3O_4 + CO \rightarrow 3\ (Mn_xFe_{1-x})O + CO_2 \quad (r6)$$

$$4\ (Mn_xFe_{1-x})_3O_4 + CH_4 \rightarrow 12\ (Mn_xFe_{1-x})O + CO_2 + 2\ H_2O \quad (r7)$$

The possibility of further reduction to MnO+Fe is feasible, but not recommended since thermodynamic restrictions would prevent complete combustion of the fuel to CO_2 and H_2O. In any case, when Fe-based oxygen carriers are used in CLC, only the transformation to Fe_3O_4 is recommended [11]. Under CLC conditions, manganese-iron mixed oxides have shown high reactivity [12] even higher than other low cost oxygen carriers already tested in the combustion of solid fuels [13]. In order to increase the mechanical stability of the manganese-iron mixed oxides, titanium oxide (TiO_2) has been used as a dopant. The addition of TiO_2 sought the formation of crystalline phases of Fe-Ti mixed oxides (ilmenite type) that improved mechanical strength of the manganese-iron particles [14]. Moreover, the addition of TiO_2 improved the cyclability with respect to the oxygen uncoupling while maintaining the magnetic properties of these materials [15] which reinforced their use in the combustion of solid fuels [16].

In the combustion of solid fuels, ashes are generated and remain in the oxygen carrier bed. Ash could have an inhibition effect resulting from ash melting/agglomeration and also deactivation of the oxygen carrier [17]. Alkali and alkaline-earth metals (AAEMs) in biomass ashes have been identified to cause this inhibition effect [18]. Thus, ashes must be periodically removed from bed, to avoid their accumulation in the CLC system and the consequences associated to it. In the drain, part of the oxygen carrier may be lost together with the ashes and this represents and extra-cost for the CLC process. Rotating fluidized beds have been proposed as a separation technique for oxygen carriers and fuel ash, but further investigation is required to apply this technology to the CLC process [19].

The magnetic properties of manganese-iron oxygen carriers would facilitate the separation of the oxygen carrier from the ash and its reuse in the system. Previous experience with this type of materials indicate that they can keep their magnetic properties after their use in the process at high temperature, under oxidizing or reducing environments. Thus, oxygen carrier particles could be recovered after cooling at room temperature using a magnetic separator and then be recycled back to the bed [20]. In a step further, it has been recently proposed the design of low reactive MnFe-based materials with magnetic properties as a support material for other highly reactive and active phase, such as CuO [21]. First tests in the combustion of both coal and biomass with this CuO oxygen carrier on a MnFe-based support indicated that the efficiency in the separation of oxygen carrier particles from fuel ash in the bed was higher than 99 % [22].

Most of the MnFe-based oxygen carriers that can be found in the literature have been prepared with commercial reagents from which formulations with different Mn-Fe molar ratios have been tested. Since one of the main costs in the CLC operation is the cost of the oxygen carrier, low-cost materials such as minerals or industrial residues are preferred to synthetic oxygen carriers [23]. However, the reactivity of low-cost materials is not always adequate to obtain high combustion efficiencies. Some studies tested specific minerals composed of manganese-iron mixed oxides. Those minerals were grinded and then directly tested as oxygen carriers. However, most of them performed poorly since they rapidly decreased their oxygen uncoupling capability and their mechanical strength with the number of cycles [24].

Considering all the above, the objective of the present work is the preparation of manganese-iron mixed oxides reinforced with titanium oxide from minerals enriched in the corresponding individual oxides (i.e. Mn_3O_4, Fe_2O_3 and TiO_2). Physicochemical characterization of

Table 1
Mn, Fe and Ti content of the minerals, as received, by ICP.

Sample	Description/Origin	% Mn	% Fe	% Ti	Other major compounds
MnSA	Mn-ore from South-Africa Supplied by FerroAtlántica del Cinca S.L.	42.1 ± 5.6	12.7 ± 3.0	<1 %	Si [(1)]
MnGBMPB	Mn-ore from Gabon Supplied by Mario Pilato Blatt	50.7 ± 2.3	2.5 ± 1.1	<1 %	Si, Al [(1)]
Tierga	Fe-ore from Spain Supplied by Promindsa	0.06±0.03	52±1.6	<1 %	Si, Ca, Al, Mg [(2)]
Ilmenite	Ore from Norway Supplied by Titania AS	<1 %	34.5 ± 2.7	25.7 ± 3.1	Si, Mg [(3)]

[(1)] Minor amounts (0.1–1 %) of Ca, K, Mg, Na, and Ti [35].
[(2)] Minor amounts (0.1–1 %) of Cr, K, and Ti [36].
[(3)] Minor amounts (0.1–1 %) of Al, Ca, Cr, Mn and V [36].

Table 2
Amounts of Mn-based minerals, Tierga and ilmenite used in the preparation of the samples and particle size after mixing and grinding.

Sample	MnSA (g)	MnGBMPB (g)	Tierga (g)	Ilmenite (g)	Mn/(Mn+Fe) molar ratio	Mn_3O_4:Fe_2O_3:TiO_2 mass fraction	Particle size (average/mode) μm
M1	40.3	–	3.3	6.4	0.66	0.60:0.33:0.07	4.2 / 3.4
M2	–	32.6	11.3	6.1	0.66	0.60:0.33:0.07	4.9 / 18
M3	43.6	–	–	6.4	0.7	0.64:0.29:0.07	5.1 / 19.8
M4	–	43.9	–	6.1	0.87	0.80:0.13:0.07	8.7 / 19.8

manganese-iron oxygen carriers with different Mn-Fe molar ratios and doped with 7 wt% TiO_2 will be done. Their reactivity will be also analysed in order to evaluate their use as oxygen carriers or as a magnetic support for more reactive active phases, as it has been previously done with synthetic oxygen carriers of this type.

2. Materials and methods

2.1. Material preparation

Four manganese-iron oxygen carriers doped with titanium were prepared from different minerals. As a source of Mn_3O_4, two minerals from South Africa (MnSA) and Gabon (MnGBMPB) were considered since they showed high reactivity in the combustion of different types of biomass [25]. The source of Fe_2O_3 was a Fe-ore denoted as Tierga that demonstrated good performance in the combustion of both coal and biomass [26,27]. Finally, the source of titanium was the mineral ilmenite, extensively used in chemical looping applications with a remarkable reactivity and durability [28–34]. Table 1 shows the ICP analysis of the minerals.

Based on results previously obtained in the research group on synthetic manganese-iron oxygen carriers, the one denoted as Mn66FeTi7 was selected to be produced from minerals due to its good performance to date [16,37]. Thus, the preparation of particles consisting of a mixed oxide with manganese to iron (Mn:Fe) molar ratio of 66:34 and doped with titanium (7 wt% TiO_2) from the abovementioned minerals was intended. Samples of manganese-iron doped with titanium were denoted as M1 to M4. M1 was produced from MnSA, Tierga and ilmenite, while sample M2 used MnGBMPB as Mn_3O_4 source. However, since ilmenite presents high iron content, it could replace Tierga as a source of Fe_2O_3, although in this case, the Mn:Fe molar ratio would be higher (see Table 2). Under this consideration, two more samples were prepared by mixing MnSA (sample M3) and MnGBMPB (sample M4) with ilmenite, respectively. In all cases, 50 g of the corresponding mixture was prepared.

Table 2 indicates the amounts of each mineral used in the preparation of samples M1 to M4, calculated according to the ICP composition shown in Table 1. Original mineral particles presented a particle size distribution between 100 and 300 μm. Once the corresponding mixture of minerals was done, it was mixed and grinded in a planetary ball mill RETSCH PM 100 in order to decrease the particle size of the mixture to less than 20 μm. It has been previously observed that pre-grinding of the mixture to low particle size was needed to form the corresponding manganese-iron mixed oxide [38].

Then, pellets of samples M1-M4 were produced by cold compression at 16 MPa for 60 s using a hydraulic press (HJE 5–5model). Cylindrical pellets (ca. 10 mm diameter, 20 mm height) were obtained and further calcined at 1050 °C for 2 h to increase their mechanical strength. Then, they were crushed and sieved to 100–300 μm.

2.2. Physic-chemical characterization of the samples

Samples M1 to M4 were characterized using different techniques. The identification of the crystalline chemical species was carried out by X-ray diffraction (XRD) in a Bruker D8 Advance X-ray powder diffractometer equipped with an X-ray source with a Cu anode working at 40 kV and 40 mA and an energy-dispersive one-dimensional detector. The diffraction pattern was obtained with a scanning rate of 0.02° over the 2θ range of 10–80°. The composition of the different materials was determined by inductively coupled plasma mass spectrometry (ICP-MS) using an ICP Jobin Ybon apparatus. Particle size distribution (PSD) of the materials was obtained in a Beckman Coulter LS13320 particle size analyzer by applying the laser diffraction technique (ISO13320 standard). The magnetic permeability was measured using a Bartington single frequency MS2G sensor connected to a magnetic susceptibility MS3 meter. Mechanical strength of the particles was determined using a Shimpo FGN-5X crushing strength apparatus. The average value of the force used to fracture the particles was obtained after at least 20 measurements.

2.3. Thermogravimetric analyzer (TGA)

The oxygen transport capacity (R_{OC}) and the oxidation and reduction rates of the samples M1 to M4 were determined using a thermogravimetric apparatus (TGA), CI Electronics type operating at atmospheric pressure. A more comprehensive description of the apparatus can be found elsewhere [39]. In all tests, approximately 50 mg of sample was used. In all cases, reduction and oxidation cycles proceed until the sample was completely reduced or oxidized, respectively.

The oxygen uncoupling capability of the MnFeTi samples was analyzed through decomposition-regeneration cycles using highly-pure N_2 (<2 ppm O_2) and air at 870 and 950 °C, respectively. The capability of the oxygen carrier materials to react with reducing gasses was also evaluated. In this case, the material can be reduced up to mangano-wüstite (MW). For that, once the desired temperature (950 °C) was reached three consecutive redox cycles were conducted alternating reduction with 15 vol.% H_2, CO or CH_4 and oxidation in air. These conditions were selected in order to compare the reactivity of the MnFeTi oxygen carriers prepared in this work with those materials prepared from highly pure Mn, Fe and Ti oxides. In order to prevent the reduction of mangano-wüstite to a mixture of MnO and metallic Fe, experiments using 5 vol.% H_2 together with a high H_2O concentration (40 vol.%) were performed. For steam addition, the gas flow was bubbled through a saturator containing water at the required temperature. The oxygen transport capacity, R_{OC}, is defined as the mass fraction that can be used in the oxygen transfer.

$$R_{OC} = \frac{m - m_r}{m_o} \tag{1}$$

where m_o and m_r are the mass of oxidized and reduced sample, respectively.

The solid conversion for the reduction, X_r, and oxidation, X_o, of the MnFeTi oxygen carriers was calculated from the mass variations registered in TGA, according to:

$$X_r = \frac{m_o - m}{R_{OC} m_o} \tag{2}$$

$$X_o = \frac{m - m_r}{R_{OC} m_o} \tag{3}$$

where m is the instantaneous mass of the sample.

Reactivity to CO and CH_4 was determined in 15 vol.% CO + 20 vol.%

Table 3
Physic-chemical characterization of oxygen carrier particles: ICP and XRD analysis, molar Mn/(Mn+Fe) ratio in the mixed oxide, purity grade of the mixed oxide in the spinel form, magnetic permeability and crushing strength.

Sample	% metal[a]			Mn/(Mn+Fe) molar ratio	% metal oxide			Purity[b]	XRD main crystalline phases[c]	Magnetic permeability (-)	Crushing strength (N)
	Mn	Fe	Ti		Mn_3O_4	Fe_3O_4	TiO_2				
M1	31.8	21.1	3.1	0.61	44.2	29.2	5.2	78.5	$(Mn_xFe_{1-x})_3O_4$, Fe_2TiO_4, $Ca_3Ti_2(Si,FeO_2)O_{12}$	2.0	5.0
M2	37.1	22.0	3.4	0.63	51.5	30.4	5.7	87.6	$(Mn_xFe_{1-x})_3O_4$, Fe_3O_4, $(Mn_xFe_{1-x})_2O_3$	1.9	5.5
M3	36.1	19.4	3.3	0.65	50.1	26.8	5.5	82.4	$(Mn_xFe_{1-x})_3O_4$, Fe_3O_4, Fe_2TiO_4, $Ca_3Ti_2(Si,FeO_2)O_{12}$	1.6	4.9
M4	48.6	10.7	3.5	0.82	67.5	14.8	5.8	88.1	$(Mn_xFe_{1-x})_2O_3$, Mn_3O_4	1.0	6.1

[a] Note that the sum of other metals different to Mn, Fe and Ti (i.e. Al, Ca, K, Mg, Na and Si) is ≤ 10 %.
[b] Purity by ICP, calculated as % Mn_3O_4+ % Fe_3O_4+ % TiO_2.
[c] $(Mn_xFe_{1-x})_3O_4$: Jacobsite/Spinel; Fe_3O_4: Magnetite; Mn_3O_4: Hausmannite; $(Mn_xFe_{1-x})_2O_3$: Bixbyite; Fe_2TiO_4: Ulvöspinel; $Ca_3Ti_2(Si,FeO_2)O_{12}$: Schorlomite.

Table 4
Theoretical and experimental oxygen transport capacity for the oxygen uncoupling reaction during N_2/air cycles performed at 870 °C and 950 °C.

Sample	$R_{OC,CLOU}$ (%)				$R_{OC,CLOU}$ (%)				Theoretical $R_{OC,CLOU}$ (%)
	870 °C				950 °C				
	N_2		O_2 (air)		N_2		O_2 (air)		
	Cycle 1	Cycle 3	Cycle 1	Cycle 3	Cycle 1	Cycle 3	Cycle 1	Cycle 3	
M1	0.14	0.15	0.21	0.20	0.17	0.13	0.14	0.12	2.67
M2	0.31	0.24	0.26	0.23	0.18	0.21	0.26	0.30	2.98
M3	0.21	0.10	0.19	0.13	0.21	0.10	0.06	0.07	2.80
M4	0.67	0.68	0.55	0.75	0.61	1.08	1.19	1.08	2.99

CO_2, or 15 vol.% CH_4 + 20 vol.% H_2O mixtures, balanced by N_2 respectively. CO_2 and H_2O were added to CO and CH_4 to prevent carbon formation in the TGA reactor [15]. The concentration of 15 vol.% was used to facilitate the reactivity comparison between different materials following the methodology based on the calculation of the rate index (RI) proposed by Johansson et al. [40]. In the case that a different gas concentration was used, the reactivity was normalized to a concentration of 15 vol.% following the same methodology. To evaluate the reaction rate of the MnFeTi-based oxygen carriers, the normalized rate index (RI) was calculated as:

$$RI\left(\frac{\%}{\min}\right) = 60 \cdot 100 \cdot \frac{P_{ref}}{P_{TGA}} \frac{1}{m_0}\left(\frac{dm}{dt}\right) \quad (4)$$

where P_{TGA} is the partial pressure of the reacting gas in TGA and P_{ref} is the reference partial pressure of the reacting gas (0.15 atm for the reduction (H_2, CO_2, or CH_4) and 0.10 atm for the oxidation (O_2). The reaction rate (dm/dt) was calculated at the beginning of the reaction.

3. Results and discussion

3.1. Characterization of the MnFeTi oxygen carriers prepared from minerals

Main results for the characterization of MnFeTi samples M1 to M4 are summarized in Table 3. ICP analysis to calcined samples allowed calculating the Mn/(Mn+Fe) ratio. As it can be seen, Mn/(Mn+Fe) ratios for samples M1 to M2 were lower than the 0.66 originally intended. Also the ratios for M3 and M4 were lower than those initially considered (0.7 and 0.87, respectively). These deviations are due to the very nature of the starting minerals where there may be a lack of homogeneity in some of their fractions. From the composition determined by ICP, the sum of Mn_3O_4, Fe_3O_4 and TiO_2 was calculated and considered as the estimated purity of the sample. In the XRD diffractograms of samples M1 to M3, the existence of the spinel phase was observed. However, in sample M4 bixbyite was detected. Spinel phase is magnetic. Then, the identified phases would explain the magnetic permeability values shown by the prepared samples in Table 3. Samples M1 to M3 present values greater than 1, indicative of their magnetic properties associated with the presence of spinel. However, sample M4 is not magnetic, since the presence of spinel is not observed. Regarding mechanical strength, samples M1 to M4 presented quite high values (≥ 5 N).

3.2. Evaluation of the oxygen uncoupling capability

As it was mentioned, the oxygen uncoupling capacity of the MnFeTi materials was evaluated in three successive reduction-oxidation cycles performed at 870 and 950 °C. This allowed the comparison with the previously developed synthetic materials. The oxygen transport capacity ($R_{OC,CLOU}$) of the first and third cycle was evaluated for each sample and results shown in Table 4 together with theoretical oxygen transport capacity values and values obtained for similar synthetic oxygen carriers.

Regardless the temperature, the capacity for oxygen uncoupling and subsequent oxidation of samples M1 to M3 was very low, especially in the case of sample M3. Values of the oxygen transport capacity were far from the theoretical values estimated. Based on this result, it will be considered that the spinel phase is not regenerated to bixbyite during oxidation and samples M1 to M3 will be further analyzed considering that spinel is the most oxidized phase. However, the behavior of sample M4 was different. It should be reminded that in this case, the Mn/(Mn+Fe) molar ratio was the highest (0.82). Sample M4 was capable of decomposing bixbyite and regenerating it at both 870 and 950 °C during the successive N_2-air cycles performed, although the oxygen transport capacity shown was almost one third the theoretical. A first indication of this capability of the sample M4 was the fact that, after calcination, sample M4 was mostly composed of bixbyite. Thus, the spinel formed during calcination at 1050 °C during 2 h was converted to bixbyite during the cooling down in the muffle in the presence of air, which would explain its lack of magnetism after calcination. Results in Table 4 for samples M1 to M4 can be compared with values in the third cycle obtained for synthetic samples with similar Mn/(Mn+Fe) ratios, i.e. Mn66FeTi7 and Mn87FeTi7 [14]. For these synthetic materials, values of $R_{OC,CLOU}$ obtained at 950 °C were 1.3 % for Mn66FeTi7 and 1.9 % for Mn87FeTi7, higher than those obtained for samples M1-M3 and M4, but

Table 5
Oxygen transport capacity for the spinel-mangano-wüstite redox system (data correspond to the third cycle).

Sample	R_{OC} (SP-MW)	R_{OC},theoretical	$X_{r,SP-MW}$(-)
M1	4.4	5.5	0.80
M2	4.1	6.1	0.67
M3	5.9	5.8	1.00
M4	5.7	6.2	0.92

also far from the theoretical for Mn66FeTi7 and Mn87FeTi7 (3.6 and 2.8 %, respectively). Although these synthetic materials presented a higher value of the molar ratio Mn/(Mn+Fe), and this was linked to a higher value of Roc,CLOU, this fact alone does not explain the low oxygen transport capacity for CLOU found for the materials prepared from minerals.

3.3. Evaluation of the reactivity with gaseous fuels

In CLC applications, reduction of spinel (SP) to manganowüstite (MW) is recommended to mostly convert the fuel to CO_2 and H_2O. In order to prevent further reduction to a mixture of MnO and metallic Fe, experiments using 5 vol.% H_2 together with a high H_2O concentration (40 vol.%) were performed at 950 °C and the oxygen transport capacity (R_{OC}) of the samples calculated in Table 5. Theoretical values were also included. The highest conversion in the transformation to manganowüstite was obtained with the samples M3 and M4, where the iron source considered was not Tierga, only iron in the corresponding manganese oxide (MnSA and MnGBMPB) and ilmenite. Thus, it seems that the spinel formed from these sources was more reactive than that formed in samples M1 and M2 in which Tierga was added.

In addition to the oxygen transport capacity of the samples, the rate index at 950 °C in the reaction with H_2, CO, CH_4 and O_2 was also calculated with the aim of comparing the samples with synthetic materials previously developed. Results are presented in Table 6 and Fig. 2. Rate indexes for the first and third cycle are shown in the table. As it can be seen in Table 6, in all cases, the first cycle always presented a lower rate index than the third, which may indicate an undergoing activation of the samples, a very common phenomenon previously observed in oxygen carriers with mineral origin [41]. This activation leads to an increase in reactivity with the number of redox cycles. The reactivity with H_2 of all the samples was of the same order, but M2 presented the lowest rate index. Similar trend was observed regarding the reactivity to CO; again, M2 was the sample with the lowest value. The reactivity to CH_4 was very low in all the cases. This has implications regarding the consideration of these materials as oxygen carriers since methane is the main volatile species present in the combustion of different types of solid fuels [42]. Thus, it is especially important that the reactivity to methane of the oxygen carrier is high to avoid the presence of unburned products at the fuel reactor outlet, which determines the efficiency of the combustion. In the case of the rate index in the reaction with oxygen, no significant differences were observed between the samples.

Fig. 2 compares the rate indexes in the third cycle obtained with M1-M4 samples with the corresponding values obtained for reference synthetic materials, i.e. Mn66FeTi7 and Mn87FeTi7 [14], considering their similarity in the Mn/(Mn+Fe) ratio. Thus, samples M1 to M3 are compared to results from sample Mn66FeTi7 and sample M4 is compared to Mn87FeTi7. Reactivity of samples M1 to M4 to H_2 was similar to that corresponding to synthetic materials although all of them were significantly more reactive to CO than the samples considered as reference. The reactivity to CH_4 and O_2 was much lower than that of synthetic Mn66FeTi7 and Mn87FeTi7. This fact, together with the low ability of the samples to regenerate from spinel to bixbyite compromise the use of the materials as oxygen carriers. Taking into account their notably high mechanical strength shown in Table 3 and principally their magnetic properties, these samples should then be also evaluated under the perspective of using them as support for other highly reactive active phases in the CLC process. As it was previously mentioned in the introduction section, the magnetism of these supports would facilitate the separation of the oxygen carrier from the fuel ashes during CLC of solid fuels. In this regard, the inertness of the support should be guaranteed, which implies assessing the lowest reactivity possible of the support under different environments [20]. In a recent study from these authors, a synthetically prepared MnFe-based mixed oxide was chosen among a portfolio to be used as support for other more reactive active phases. The selection was made based on mechanical properties and reactivity under oxidizing and reducing environments. Rate indexes for decomposition-regeneration of the bixbyite at 880 °C and for spinel reduction to mangano-wüstite with H_2 at 950 °C were calculated for all the MnFe-based materials considered. The material finally chosen as potential magnetic support (MnFe50–1200) presented rate values of 0.3 %/min for bixbyte regeneration at 880 °C and 6.5 %/min at 950 °C in the SP-MW reduction at 950 °C. Besides, its value of crushing strength was 4.0 N. Taking the previous rate indexes as reference of inertness for a potential MnFe-based magnetic support, the sample from M1-M4 that better combines high inertness under oxidizing and reducing conditions is sample M2. This sample was not capable of significantly oxidize from spinel to bixbyite at 870 °C (very low oxygen uncoupling capability) and showed the lowest reactivity in the conversion of spinel to

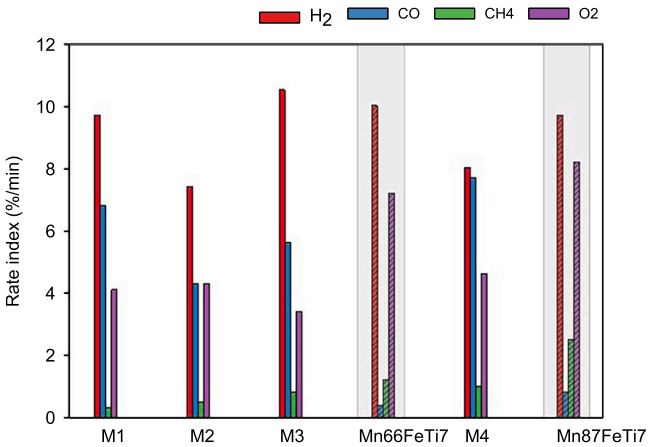

Fig. 2. Rate index /%/min) with different gasses at 950 °C of samples M1 to M4. Results for similar synthetic materials included for comparison [14].

Table 6
Rate index of MnFe materials prepared from minerals with different gasses at 950 °C.

Sample	Rate Index (%/min)							
	H_2		CO		CH_4		O_2	
	Cycle 1	Cycle 3	Cycle 1	Cycle 3	Cycle 1	Cycle 3	Cycle 1	Cycle 3
M1	2.1	9.7	2.2	6.8	0.1	0.3	2.6	4.1
M2	2.5	7.4	1.3	4.3	0.2	0.5	3.3	4.3
M3	1.6	10.5	2.1	5.6	0.1	0.8	2.1	3.4
M4	3.4	8.0	1.9	7.7	0.1	1.0	4.2	4.6

Table 7
Main physical properties of Cu30_MIN and Cu30_Support_1030.

Sample	Crushing strength (N)		Magnetic permeability (-)		Rate index[a] (%/min)	X_r[a] (-)
	Fresh	Used	Fresh	Used		
Cu30_MIN	2.2	1.6	2.4	1.5	1.24	0.84
Cu30_Support_1030	2.0	–	2.6	–	0.4	0.62

[a] After 3 N_2-air cycles in TGA at 950 °C.

manganowüstite in the reaction with the main gasses in combustion at high temperatures. As it was shown in Table 3, M2 also presented high values of mechanical strength and magnetic permeability. Thus, sample M2 was selected as potential support material.

3.4. Preparation of a Cu-based oxygen carrier with sample M2 as support

As it has been previously mentioned, in CLC of solid fuels, the use of oxygen carriers with magnetic properties has been proposed as one alternative to easily remove the fuel ashes from the oxygen carrier bed and facilitate the recovery of the oxygen carrier material lost in this drainage [20]. Moreover, CLC of solid fuels is facilitated when oxygen carriers with the ability to release molecular oxygen are used. Oxygen carriers operating under the Chemical Looping with Oxygen Uncoupling (CLOU) mechanism release oxygen that directly reacts with both volatiles and the fuel char, significantly reducing the amount of unburned products of combustion and therefore enhancing both combustion efficiency and CO_2 capture efficiency [42]. Among the oxygen carriers commonly used in CLOU, CuO-based materials have demonstrated high oxygen release rate and high CLOU transport capacity [43,44]. Recently, CuO-based oxygen carrires were prepared using a magnetic MnFe-based support with good performance in the combustion of both coal and biomass [22]. Then, in order to assess the possibility of replicating this type of materials using a magnetic MnFe support prepared from minerals, sample M2 was used as support in the replication of this CuO-based oxygen carrier previously developed by the authors from exclusively synthetic sources.

The new oxygen carrier was prepared mixing sample M2 with CuO from CHEMLAB so that CuO represented 30 wt.%. Thus, the corresponding amounts of MnGBMPB, Tierga and ilmenite were mixed with CuO particles and mixed/milled in a RETSCH mill at 90 rpm. The final size of the mixture was <10 μm to facilitate the formation of spinel phases. The mixture was then pelletized by compression and the obtained pellets calcined at 1050 °C during 2 h. After calcination pellets were milled to fluidizable size (100–300 μm). The oxygen carrier obtained was noted as Cu30_MIN,

As it is shown in Table 7, the oxygen carrier Cu30_MIN presented high mechanical strength after calcination (2.2 N) and magnetic properties (magnetic permeability is 2.4). Values obtained for Cu30_MIN were also compared in Table 7 with those found for a similar CuO-based material (30CuO_Support_1030) also prepared by pelletization by Adánez et al. [21] but using synthetic sources. The previously mentioned 30CuO_Support_1030 presented similar values of crushing strength and magnetic permeability to Cu30_MIN.

XRD patterns of both Cu30_MIN and 30CuO_Support_1030 were

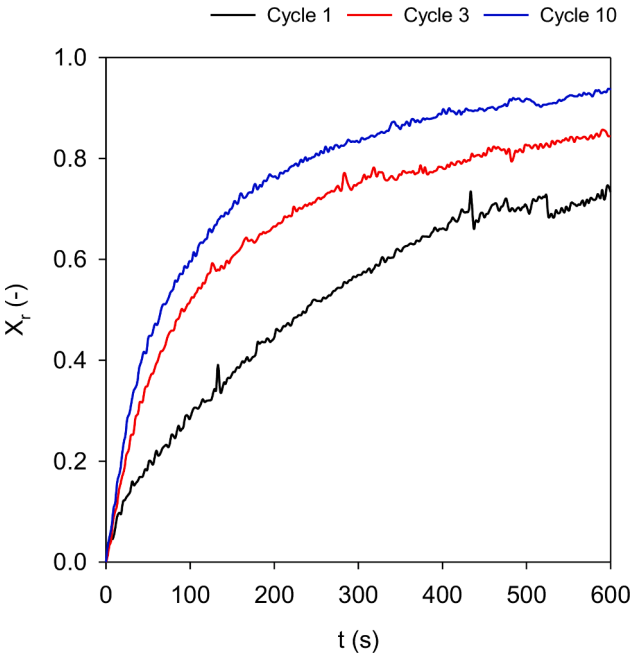

Fig. 4. Reduction conversion with time for Cu30_MIN in 10 N_2-air cycles at 950 °C.

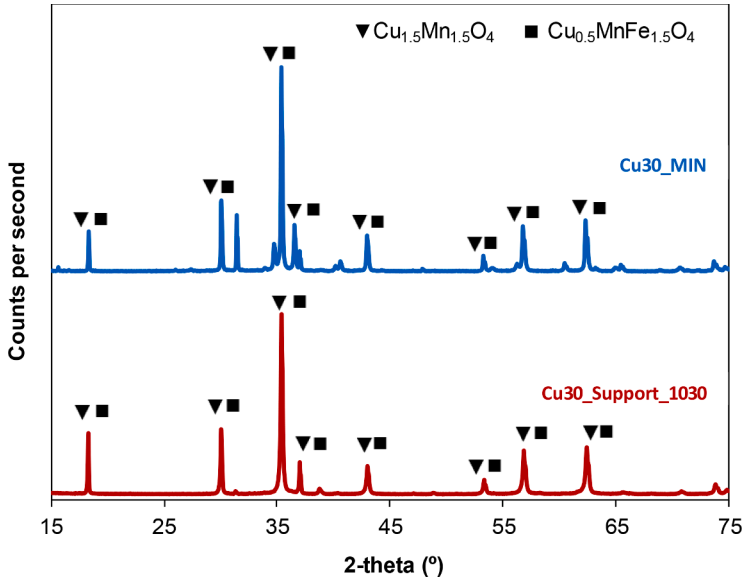

Fig. 3. XRD patterns of Cu30_MIN and Cu30_Support_1030.

obtained and compared in Fig. 3. The main mixed oxides identified by XRD according to a reference pattern database compiled from the Crystallography Open Database (COD) and The Powder Diffraction File (PDF) were $Cu_{1.5}Mn_{1.5}O_4$ and $Cu_{0.5}MnFe_{1.5}O_4$. Both are thought to release O_2 under CLOU conditions. As it can also be seen in Fig. 3, some unidentified peaks appear in the XRD pattern corresponding to Cu30_MIN. They are thought to be phyllosilicates present in this sample due to its mineral origin. Despite the intensity of these peaks they can be considered only as impurities and they do not participate in the oxygen transfer during CLC.

The reactivity of the Cu30_MIN oxygen carrier was evaluated in ten N_2-air cycles at 950 °C. Fig. 4 shows the evolution of the reduction conversion with time for the N_2-air cycles performed.

The reactivity of the sample increased with the number of cycles. The conversion reached by the sample Cu30_MIN in the tenth cycle and after ten minutes of reaction was 0.94. The rate index increased with the number of cycles from 0.61 %/min in cycle 1, to 1.24 %/min in cycle 3 and to a final rate index of 1.44 %/min in cycle 10. Table 7 also shows how this increase in reactivity was accompanied by a decrease of the crushing strength to 1.6 N. It should be reminded that values higher than 1 N are necessary for operation in a fluidized bed. If reactivity results for Cu30_MIN are compared to those of Cu30_Support_1030 in Table 7, it can be observed that the rate index at 950 °C for Cu30_MIN was three times higher than the corresponding value reported for the synthetic oxygen carrier. Moreover, if the third cycle is compared for both Cu30_MIN and Cu30_Support_1030, after 10 min of reaction in N_2, the first reached a reduction conversion value of 0.84 and the latter 0.62. Finally in Table 7, the magnetic permeability of Cu30_MIN also decreased after TGA N_2-air cycles, but the used sample kept its magnetic properties. This decrease in the magnetic susceptibility has also been observed in used synthetic samples of similar composition to that of Cu30_MIN [22]. Thus, it can be concluded that the synthetic material 30CuO_Support_1030 could be replicated using a support developed from the combination of minerals enriched in manganese, iron and titanium.

5. Conclusions

Four samples composed of manganese-iron mixed oxide doped with titanium were developed from minerals enriched in manganese, iron and titanium, using molar Mn/(Mn+Fe) ratios between 0.61–0.82. The samples aim at replicating similar manganese-iron based synthetic materials previously developed by the authors and successfully tested as oxygen carriers in the combustion of mainly solid fuels.

The mechanical properties and the reactivity of the samples produced from minerals was evaluated. All of them showed high crushing strength and magnetic properties. The reactivity was evaluated in a TGA. N_2-air cycles were performed to analyze the oxygen uncoupling capability of the materials. Reaction with H_2, CO and CH_4 was also investigated. The samples showed very low oxygen uncoupling capability and also low reactivity in the reaction with H_2, CO and CH_4. Thus, their use as magnetic support for other active phases was considered. In this regard, a CuO based oxygen carrier was prepared supporting 30 wt. %. CuO on one of the manganese-iron materials developed from minerals (Cu30_MIN). The Cu30_MIN oxygen carrier showed similar properties and reactivity to a previously developed synthetic material (Cu30_Support_1030), which opens the possibility of developing low-cost magnetic oxygen carriers with oxygen release capacity.

CRediT authorship contribution statement

Beatriz Zornoza: Conceptualization, Data curation, Formal analysis, Investigation, Methodology, Validation. **Teresa Mendiara:** Conceptualization, Data curation, Investigation, Methodology, Supervision, Validation, Visualization, Writing – original draft, Writing – review & editing. **Alberto Abad:** Conceptualization, Data curation, Funding acquisition, Methodology, Project administration, Resources, Supervision, Validation, Visualization.

Declaration of Competing Interest

The authors declare that they have no known competing financial interests or personal relationships that could have appeared to influence the work reported in this paper.

Data availability

Data will be made available on request.

Acknowledgment

This work was supported by Grant PDC2021-121190-I00 MCIN/AEI/10.13039/501100011033 and European Union NextGenerationEU/PRTR. The authors thank Ferroatlántica del Cinca (former Hidro Nitro Española S.A) for providing MnSA; Mario Pilato Blatt S.A. for providing MnGBMPB, PROMINDSA for providing Tierga ore and Titania for providing ilmenite. B.Z. acknowledges the “Juan de la Cierva” Program (IJCI-2016–30776).

References

[1] EU, 2019. Communication from the commission to the European parliament, the European council, the council, the European economic and social committee and the committee of the regions. The European Green Deal., COM/2019/640 final.
[2] ONU. United nations framework convention for climate change. Paris Agreement. 2015 http://unfccc.int/paris_agreement/items/9485.php.
[3] Pisciotta M, Pilorge H, Feldmann J, Jacobson R, Davids J, Swett S, et al. Current state of industrial heating and opportunities for decarbonization. Prog Energy Combust Sci 2022;91:100982.
[4] Adanez J, Abad A, Garcia-Labiano F, Gayan P, De Diego LF. Progress in chemical-looping combustion and reforming technologies. Prog Energy Combust Sci 2012;38(2):215–82.
[5] Abuelgasim S, Wang WJ, Abdalazeez A. A brief review for chemical looping combustion as a promising CO_2 capture technology: fundamentals and progress. Sci Total Environ 2021;764:142892.
[6] Lewis WK, Gilliland ER. Production of pure carbon dioxide. S.O.D. Company, US Patent; 1954. 2,665,971.
[7] Daneshmand-Jahromi S, Sedghkerdar MH, Mahinpey N. A review of chemical looping combustion technology: fundamentals, and development of natural, industrial waste, and synthetic oxygen carriers. Fuel 2023;341:127626.
[8] Azimi G, Leion H, Rydén M, Mattisson T, Lyngfelt A. Investigation of different Mn-Fe oxides as oxygen carrier for chemical-looping with oxygen uncoupling (CLOU). Energy Fuels 2013;27(1):367–77.
[9] Larring Y, Braley C, Pishahang M, Andreassen KA, Bredesen R. Evaluation of a mixed Fe-Mn oxide system for chemical looping combustion. Energy Fuels 2015;29(5):3438–45.
[10] Pérez-Vega R, Abad A, Gayán P, de Diego LF, García-Labiano F, Adánez J. Development of $(Mn_{0.77}Fe_{0.23})_2O_3$ particles as an oxygen carrier for coal combustion with CO_2 capture via *in-situ* gasification chemical looping combustion (iG-CLC) aided by oxygen uncoupling (CLOU). Fuel Process Technol 2017;164:69–79.
[11] Jerndal E, Mattisson T, Lyngfelt A. Thermal analysis of chemical-looping combustion. Chem Eng Res Des 2006;84(9 A):795–806.
[12] Moldenhauer P, Serrano A, Garcia-Labiano F, de Diego LF, Biermann M, Mattisson T, Lyngfelt A. Chemical-looping combustion of kerosene and gaseous fuels with a natural and a manufactured Mn-Fe-based oxygen carrier. Energy Fuels 2018;32(8):8803–16.
[13] Pérez-Vega R, Abad A, García-Labiano F, Gayán P, de Diego LF, Izquierdo MT, Adánez J. Chemical looping combustion of gaseous and solid fuels with manganese-iron mixed oxide as oxygen carrier. Energy Convers Manag 2018;159:221–31.
[14] Abián M, Abad A, Izquierdo MT, Gayán P, de Diego LF, García-Labiano F, Adánez J. Titanium substituted manganese-ferrite as an oxygen carrier with permanent magnetic properties for chemical looping combustion of solid fuels. Fuel 2017;195:38–48.
[15] Pérez-Vega R, Abad A, Izquierdo MT, Gayán P, de Diego LF, Adánez J. Evaluation of Mn-Fe mixed oxide doped with TiO_2 for the combustion with CO_2 capture by chemical looping assisted by oxygen uncoupling. Appl Energy 2019;237:822–35.
[16] Pérez-Vega R, Abad A, Gayán P, García-Labiano F, Izquierdo MT, de Diego LF, et al. Coal combustion via chemical looping assisted by oxygen uncoupling with a manganese-iron mixed oxide doped with titanium. Fuel Process Technol 2020;197:106184.

[17] Liu Y, Yin K, Wu J, Mei D, Konttinen J, Joronen T, et al. Ash chemistry in chemical looping process for biomass valorization. Rev Chem Eng J 2023;478:147429.
[18] Stanicic I, Hanning M, Deniz R, Mattisson T, Backman R, Leion H. Interaction of oxygen carriers with common biomass ash components. Fuel Process Technol 2020;200:106313.
[19] Weber JM, Stehle RC, Breault RW, De Wilde J. Experimental study of the application of rotating fluidized beds to particle separation. Powder Technol 2017; 316:123–30.
[20] Abad A, Perez-Vega R, Izquierdo MT, Gayan P, Garcia-Labiano F, de Diego LF, et al. Novel magnetic manganese-iron materials for separation of solids used in high-temperature processes: application to oxygen carriers for chemical looping combustion. Fuel 2022;320:123901.
[21] Adanez-Rubio I, Bautista H, Izquierdo MT, Gayan P, Abad A, Adanez J. Development of a magnetic Cu-based oxygen carrier for the chemical looping with oxygen uncoupling (CLOU) process. Fuel Process Technol 2021;218:106836.
[22] Adanez-Rubio I, Sampron I, Izquierdo MT, Abad A, Gayan P, Adanez J. Coal and biomass combustion with CO_2 capture by CLOU process using a magnetic Fe-Mn-supported CuO oxygen carrier. Fuel 2022;314:122742.
[23] Lyngfelt A, Leckner B. A 1000 MW_{th} boiler for chemical-looping combustion of solid fuels - discussion of design and costs. Appl Energy 2015;157:475–87.
[24] Larring Y, Pishahang M, Sunding MF, Tsakalakis K. Fe-Mn based minerals with remarkable redox characteristics for chemical looping combustion. Fuel 2015;159: 169–78.
[25] Pérez-Astray A, Mendiara T, de Diego LF, Abad A, García-Labiano F, Izquierdo MT, et al. Improving the oxygen demand in biomass CLC using manganese ores. Fuel 2020;274:117803.
[26] Mendiara T, Abad A, de Diego LF, García-Labiano F, Gayán P, Adánez J. Biomass combustion in a CLC system using an iron ore as an oxygen carrier. Int J Greenh Gas Control 2013;19:322–30.
[27] Mendiara T, De Diego LF, García-Labiano F, Gayán P, Abad A, Adánez J. On the use of a highly reactive iron ore in chemical looping combustion of different coals. Fuel 2014;126:239–49.
[28] Condori O, Abad A, Izquierdo MT, de Diego LF, Garcia-Labiano F, Adanez J. Assessment of the chemical looping gasification of wheat straw pellets at the 20 kW_{th} scale. Fuel 2023;344:128059.
[29] Kolbitsch P, Bolhar-Nordenkampf J, Proll T, Hofbauer H. Operating experience with chemical looping combustion in a 120kW dual circulating fluidized bed (DCFB) unit. Int J Greenh Gas Control 2010;4(2):180–5.
[30] Markström P, Linderholm C, Lyngfelt A. Operation of a 100kW chemical-looping combustor with Mexican petroleum coke and Cerrejón coal. Appl Energy 2014; 113:1830–5.
[31] Pérez-Vega R, Abad A, García-Labiano F, Gayán P, de Diego LF, Adánez J. Coal combustion in a 50 kW_{th} chemical looping combustion unit: seeking operating conditions to maximize CO_2 capture and combustion efficiency. Int J Greenh Gas Control 2016;50:80–92.
[32] Ströhle J, Orth M, Epple B. Design and operation of a 1 MW_{th} chemical looping plant. Appl Energy 2014;113:1490–5.
[33] Ströhle J, Orth M, Epple B. Chemical looping combustion of hard coal in a 1 MW_{th} pilot plant using ilmenite as oxygen carrier. Appl Energy 2015;157:288–94.
[34] Thon A, Kramp M, Hartge EU, Heinrich S, Werther J. Operational experience with a system of coupled fluidized beds for chemical looping combustion of solid fuels using ilmenite as oxygen carrier. Appl Energy 2014;118:309–17.
[35] Mei D, Mendiara T, Abad A, De Diego LF, García-Labiano F, Gayán P, Adánez J, Zhao H. Evaluation of manganese minerals for chemical looping combustion. Energy Fuels 2015;29(10):6605–15.
[36] Mendiara T, Gayán P, Abad A, García-Labiano F, de Diego LF, Adánez J. Characterization for disposal of Fe-based oxygen carriers from a CLC unit burning coal. Fuel Process Technol 2015;138:750–7.
[37] Perez-Astray A, Mendiara T, de Diego LF, Abad A, Garcia-Labiano F, Izquierdo MT, et al. Behavior of a manganese-iron mixed oxide doped with titanium in reducing the oxygen demand for CLC of biomass. Fuel 2021;292:120831.
[38] Zornoza B, Mendiara T, Abad A. Evaluation of oxygen carriers based on manganese-iron mixed oxides prepared from natural ores or industrial waste products for chemical looping processes. Fuel Process Technol 2022;234:107313.
[39] De Diego LF, Abad A, Cabello A, Gayán P, García-Labiano F, Adánez J. Reduction and oxidation kinetics of a $CaMn_{0.9}Mg_{0.1}O_{3-\delta}$ oxygen carrier for chemical-looping combustion. Ind Eng Chem Res 2014;53(1):87–103.
[40] Johansson M, Mattisson T, Lyngfelt A. Investigation of Mn_3O_4 with stabilized ZrO_2 for chemical-looping combustion. Chem Eng Res Des 2006;84(9 A):807–18.
[41] Mendiara T, Pérez R, Abad A, De Diego LF, García-Labiano F, Gayán P, Adánez J. Low-cost Fe-based oxygen carrier materials for the *i*G-CLC process with coal. 1. Ind Eng Chem Res 2012;51(50):16216–29.
[42] Adánez J, Abad A, Mendiara T, Gayán P, de Diego LF, García-Labiano F. Chemical looping combustion of solid fuels. Prog Energy Combust Sci 2018;65:6–66.
[43] Adánez-Rubio I, Abad A, Gayán P, de Diego LF, García-Labiano F, Adánez J. Performance of CLOU process in the combustion of different types of coal with CO_2 capture. Int J Greenh Gas Control 2013;12:430–40.
[44] Adánez-Rubio I, Abad A, Gayán P, De Diego LF, García-Labiano F, Adánez J. Biomass combustion with CO_2 capture by chemical looping with oxygen uncoupling (CLOU). Fuel Process Technol 2014;124:104–14.